Current Controlled Vented Box Loudspeaker System with Motional Feedback

5110 (G - 5)

Philippe Robineau (1) and Mario Rossi (2),
(1) TANNOY, Coatbridge Strathclyde, Scotland, UK
(2) Federal Institute of Technology EPFL, Lausanne, Switzerland

Presented at
the 108th Convention
2000 February 19-22
Paris, France

AES

AN AUDIO ENGINEERING SOCIETY PREPRINT

Current controlled vented box loudspeaker system with motional feedback

*Philippe Robineau *and Mario Rossi***

**TANNOY*
Rosehall Industrial Estate, Coatbridge Strathclyde ML5 4 TF, Scotland, UK

***Laboratory of Electromagnetism and Acoustics (LEMA)*
Federal Institute of Technology (EPFL), CH-1015 Lausanne, Switzerland
mario.rossi@epfl.ch

Abstract: To obtain a very stable response in the whole range of operating conditions combined with high acoustic output we designed a current controlled vented box loudspeaker system. To overcome the drawbacks of current control - response underdamped and sensitive to the mechanical parameters - we implemented motional feedback with a secondary coil sensing the velocity. We checked that a vented system was applicable.

Introduction

This paper deals with the design and implementation of current controlled open box loudspeaker systems with motional feedback. Such systems were required in the field of outdoor active noise control technologies. In comparison with standard audio problems, the far field requirement on the phase response, which needs to be completely controlled, over and above the requirement of a suitable amplitude response, led to the loudspeaker analysis and synthesis methods being reconsidered and adapted (see paper by V. Adam: amplitude and phase synthesis of loudspeaker systems).

The demand for a very stable response - both in amplitude and phase- in the whole range of operating conditions, combined with a high acoustic output, appeared to be especially difficult to achieve. One fundamental problem was indeed the phenomenon of power compression which is known to effect significantly the performances of conventional drivers as the temperature of the voice coil varies. Based on simulations it was predicted that the variations in amplitude could be as high as 4 dB, which was unacceptable. Different methods were studied to overcome this, amongst which the "current drive" technology, which was selected as being the most reliable. This technology

brings the benefit of a response that is independent of the coil DC resistance - therefore of its temperature - but it also has a few drawbacks as a result of the absence of electrical damping :

a) the response is highly underdamped in the bottom end and requires a correction

b) the response becomes very sensitive to variations in the mechanical parameters that are difficult to control.

A theoretical solution to eliminate or greatly reduce these problems is to use motional feedback. A study was carried out on the feasibility of implementing it, leading us to choose the solution of a secondary coil sensing the velocity (as reflected by its back *e.m.f.* proportional to the (*Bl*) product of the magnetic gap).

During the preliminary phase, the requirements for the sources were translated into actual specifications, making sure they would be relevant and meaningful in relation to the manufacturing of the loudspeakers. Table 1 summarises the specifications. The outdoor use required protection both against bad weather and UV's. Furthermore, size and weight had to be kept as low as possible. From this point the development was divided into two sub-sections: driver and system alignment on the one hand, current drive amplification on the other hand.

Driver Design

The first stage of the driver design was to assess a number of basic specifications such as size, materials, etc. From the peak output power and the low frequency extension specified one could deduce a requirement for a volume of air to be displaced equivalent to 300 cm^3, for which we selected a driver size of 12" (30 cm) providing a radiating area of 0.0530 cm^2 . The peak displacement is about 5.6 mm. For a 15'' driver, the size would have been too great, whereas for a 10'' driver, the displacement would have been too high (8.8 mm). Among all the materials available for the cone, it appeared that injection moulded polypropylene would be the ideal choice, given the outdoor conditions where the driver has to operate. The cone is coupled to a rubber surround, a classic material again offering the benefit of true waterproofness and durability. The moving coil has a diameter of 51 mm, fixed according to its thermal behaviour (dissipation) and in relation to the possibility of assembling it with the plastic. Three successive generations of prototypes were developed before we got to a satisfactory set of performances, each one including new refinements especially in the magnet design which was crucial in order to keep the non-linearity to a minimum for the specified value of Bl product.

System Design

Before proceeding further with the detailed cabinet design, it had to be checked that a vented system was applicable here, as per use with a current drive and motional feedback. A vented system seemed to be of more interest than a closed box, because it is intrinsically more efficient and has a smaller displacement. However, it has a greater group delay. Such a configuration had not been studied in existing literature, a preliminary academic work had therefore to be carried out. This work showed the relevance of this electroacoustic architecture and brought a number of results to be used for the ensuing development stage. The actual enclosure design was then started, the aim being to optimise internal volume, port tubes / tuning frequency, cabinet shape, internal damping, etc...

The tuning frequency f_b of the box was fixed at 65 Hz, which led to a group delay of less than 5 ms being achieved.

Figures 1 and 2 show the complete and simplified circuit diagrams of current-controlled vented loudspeaker system. It is from the simplified circuit that the loudspeaker and its vented box were designed.

Current Drive Design

On the other hand, development on current drive technology started with an extensive investigation of various topologies achieving a transconductance power source. Eventually the simplest topology, using a single sensing series resistor and a properly band limited feedback loop, proved to be the most effective for this application. After it had been successfully implemented, the next step was to incorporate the motional feedback loop according to Figure 3. Figures 4 and 5 exhibit the two feedback principles studied: with a single series resistance and the Howland circuit. Figures 6 and 7 show the behaviour of these circuits for different values of load impedance Z_L. A number of possible ways of applying the feedback were assessed, from purely velocity to purely acceleration including a combination of both and filtering sections. Figures 8 and 9 show different frequency responses with various feedback controls (velocity or acceleration). This process was optimised experimentally with the actual prototype loudspeaker. Finally, an equalisation section was added to smooth the on-axis response of the loudspeaker up to 2 kHz, making the task of the digital control unit easier. Figure 10 shows the final circuit, the amplitude and phase responses of which are given in Figure 11. Figure 12 exhibits the transconductance modulus and phase as a function of frequency and Figure 13 shows the complete bloc diagram with feedback loop. All these electronic sections have been implemented on a single PCB, with connections to the driver and to a conventional voltage amplifier providing the power stage. Because of the very

high power demanded for this power stage it was decided to use a suitably selected off-the-shelf amplifier rather than to design and build our own from scratch with no real benefit.

Implementation and Performances

Final prototypes were tested in terms of acoustic response, directivity, and non-linearity. For the latter we used noise records and set up a calibrated coherence measurement using a dual channel FFT analyser. In all respects the loudspeaker was found to comply with the specifications.

Figure 14 exhibits the amplitude frequency response and figure 15 shows the group delay as a function of frequency in conjunction with the current and voltage control. The curves in figure 16 illustrate the effects of the thermal compression with and without feedback. Figures 17 and 18 show the THD distortion measurement results. The evaluation of non-linearity effects was also carried out using recordings of aeroplane noise corresponding to the primary noise source to be counteracted. Values of the order of 0.95 were obtained (95 % of the output is coherent with the input, 5 % is noise or resulting distortion). In this case we measured the Coherence which expresses the degree of linearity between the input and output of a system. Dans ce cas nous avons mesuré la Cohenrece qui exprime le degree de linéarité entre sortie d'un système.

A certain number of improvements are envisaged:

- increase in the efficiency using a more powerful magnet (neodym)
- improvement in the heat transfer through the use of forced convection in the air-gap
- improvement in the linearity using an accelerometer instead of a second coil.
- with a view of reducing the cost, introduction of a class D amplifier.

In conclusion, the generalisation of current control in association with motional feedback to loudspeaker systems of the 3rd order or higher, opens up interesting perspectives for other applications for which the reduction of compression-related effects is a crucial requirement (high power sound reinforcement, for example).

- Low frequency cut-off ≤ 100 Hz
- High frequency cut-off ≥ 1000 Hz
- Peak acoustic power 12.6 W
- Peak factor 11 dB
- Peak SPL at 1 m 120 dBSPL
- RMS SPL at 1 m 109 dBSPL
- Group delay ≤ 5 ms
- Non-linearity effects ≤ -30 dB
- Available volume about 30 l
- Resistant to bad weather and UV rays
- Ambient temperature range 0° - 40°
- Tolerance between sources ≤ ± 0.5 dB

Table 1 – Specifications

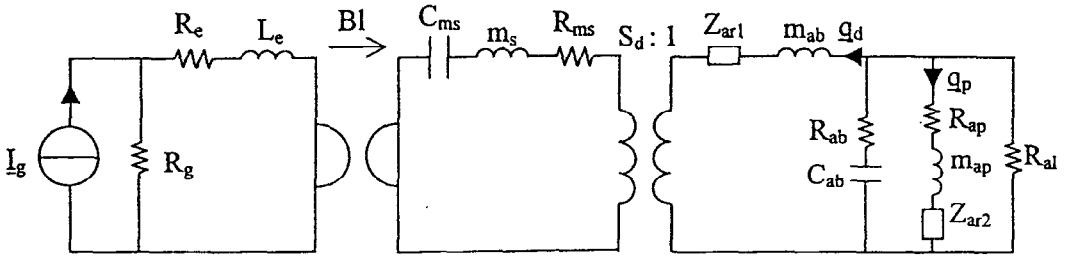

Figure 1 – Electro-mechano-acoustic circuit diagram of current-controlled vented loudspeaker system.

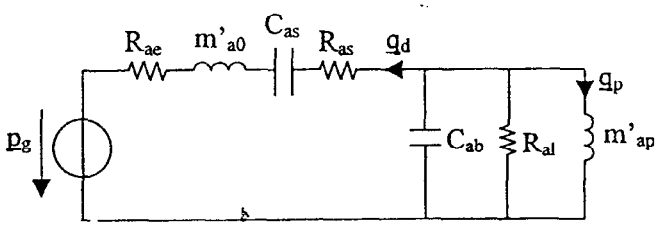

Figure 2 – Simplified low-frequency acoustic circuit diagram

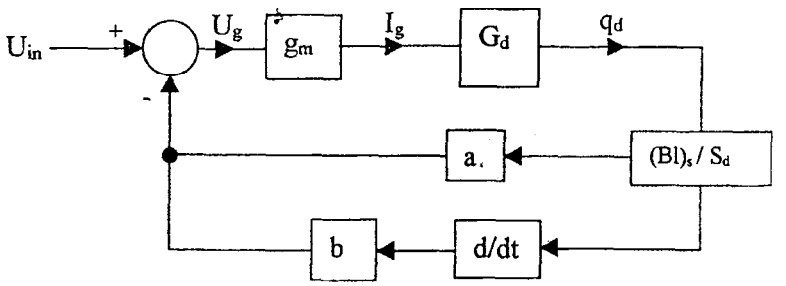

Figure 3 – Motional feedback bloc diagram

U_{in} [V]	control voltage of the complete system with feedback (information signal with the noise to be transmitted)
U_g [V]	control voltage of the current output amplifier
G_m [A/V]	transconductance of the current output amplifier (internal to the system)
I_g [A]	current delivered by the power amplifier to the loudspeaker
G_d [m^3/sA]	transfer function linking the volume velocity q_d of the diaphragm to the current I_g delivered by the loudspeaker amplifier
$(BL)_s$ [N/A]	force per unit of current developed by the velocity measurement coil
a	velocity feedback gain
b	acceleration feedback gain

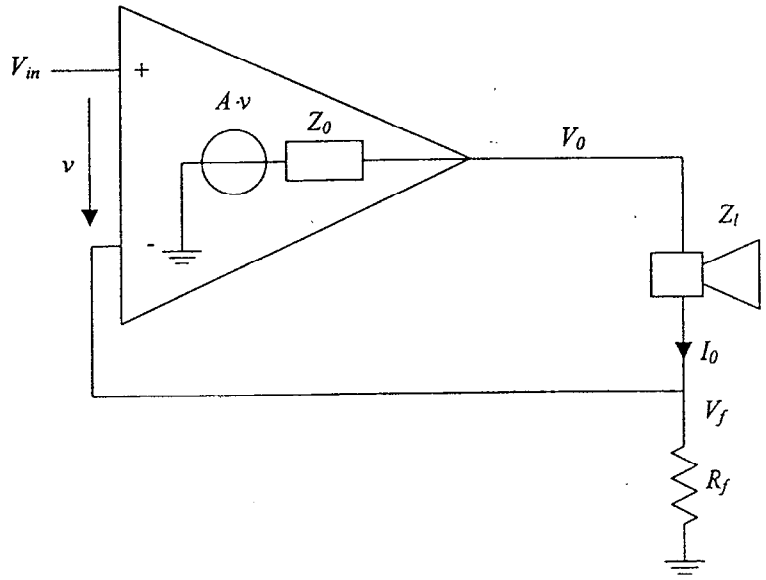

$$g_m = Io / V_{in} = A / \{ R_f (1 + A) + Zo + Z_l \}$$

$$Z_{out} = - [R_f (1 + A) + Zo]$$

Figure 4 – Current feedback circuit

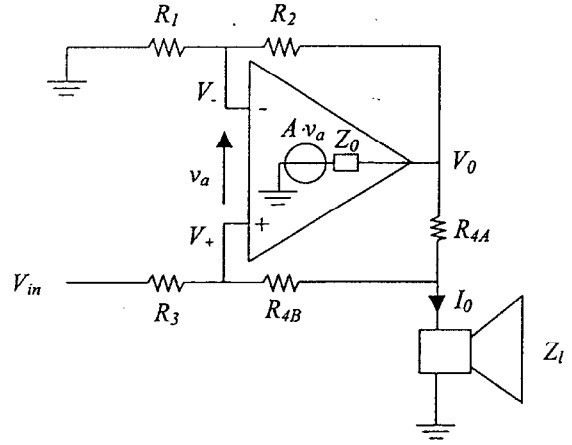

$$g_{mHowland} = \frac{A\left[R_1\left(R_{4A}+R_{4B}\right)+R_2R_{4B}\right]+\left(Z_0R_{4A}\right)\left(R_1+R_2\right)+Z_0R_{4A}}{A\left[Z_L\left(R_1\left(R_{4A}+R_{4B}\right)-R_2R_3\right)+R_1R_{4A}\left(R_3+R_{4B}\right)\right]+Z_LZ_0\left(R_{4A}+R_{4B}\right)}$$

$$Z_{OutHowland} = \frac{AR_1R_{4A}\left(R_3+R_{4B}\right)+\left(R_3+R_{4B}\right)\left[\left(R_1+R_2\right)\left(Z_0+R_{4A}\right)+Z_0R_{4A}\right]}{A\left[R_1\left(R_{4A}+R_{4B}\right)-R_2R_3\right]+\left(R_1+R_2+Z_0\right)\left(Z_0+R_3+R_{4A}+R_{4B}\right)-Z_0^2}$$

Figure 5– Howland circuit

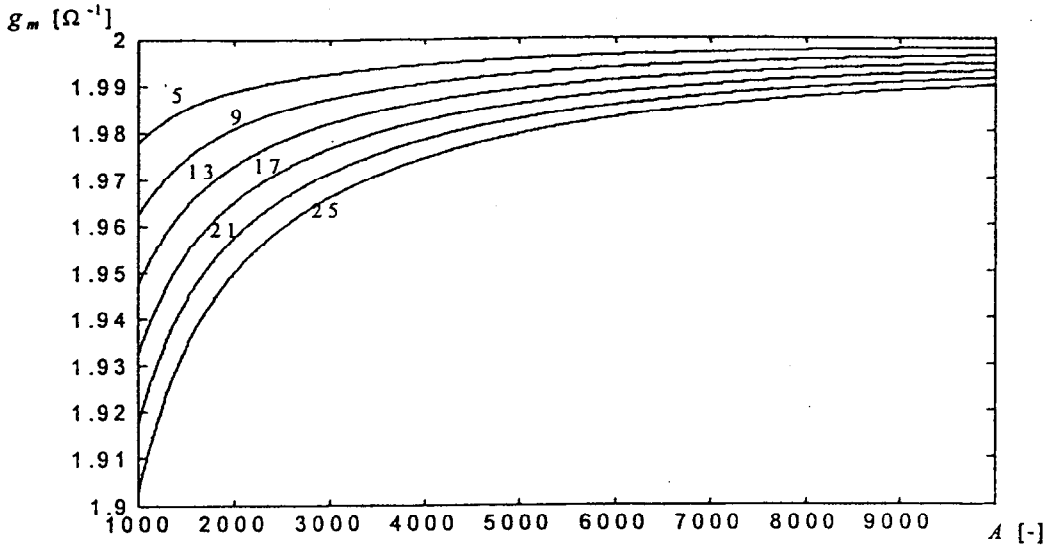

Figure 6 – Behaviour of current feedback circuit

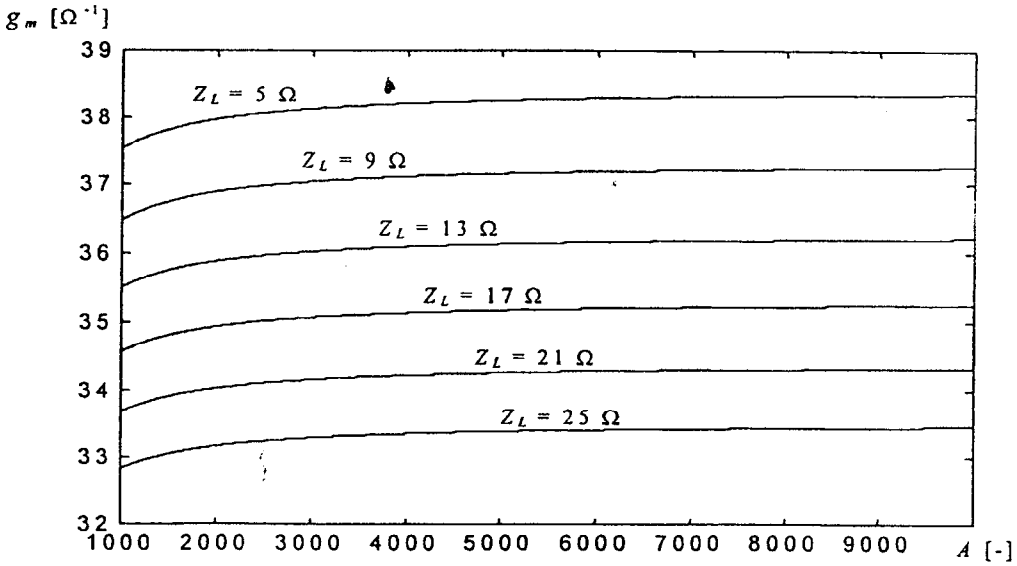

Figure 7 – Behaviour of Howland circuit

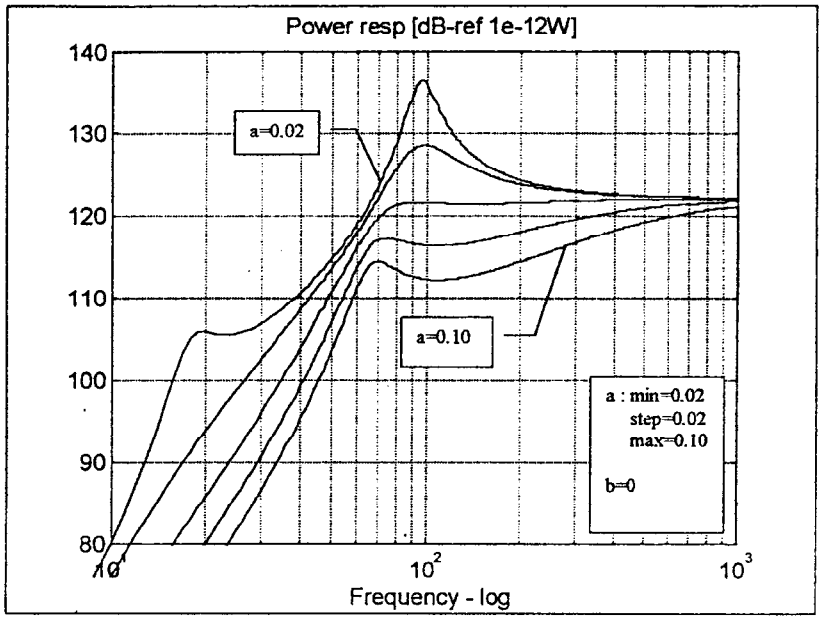

Figure 8 – Outline of frequency responses with velocity feedback only

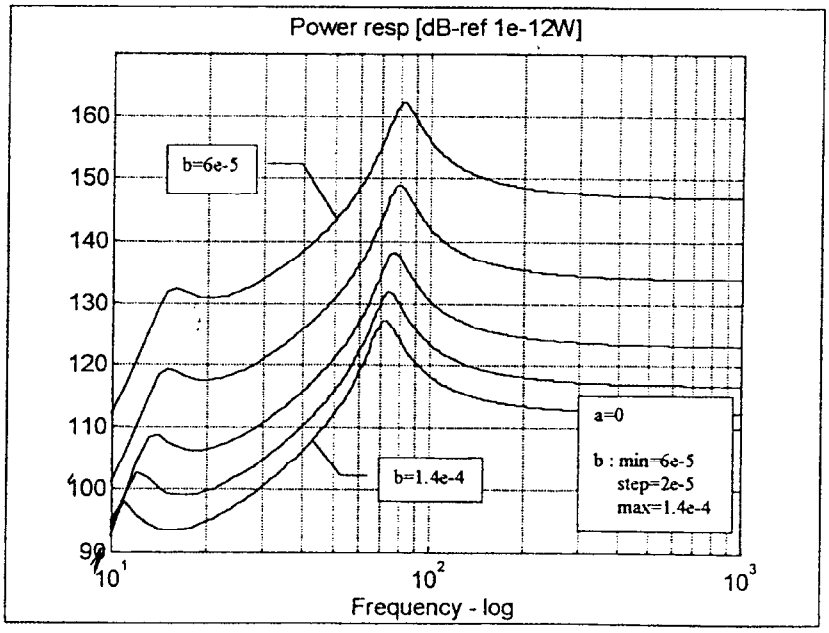

Figure 9 – Outline of frequency responses with acceleration feedback only

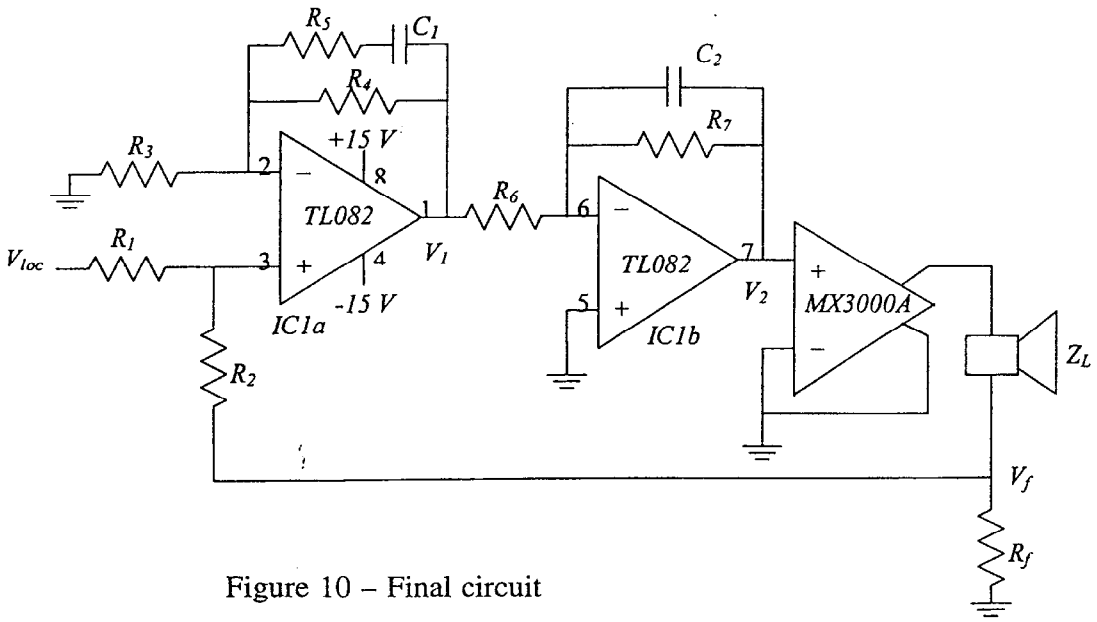

Figure 10 – Final circuit

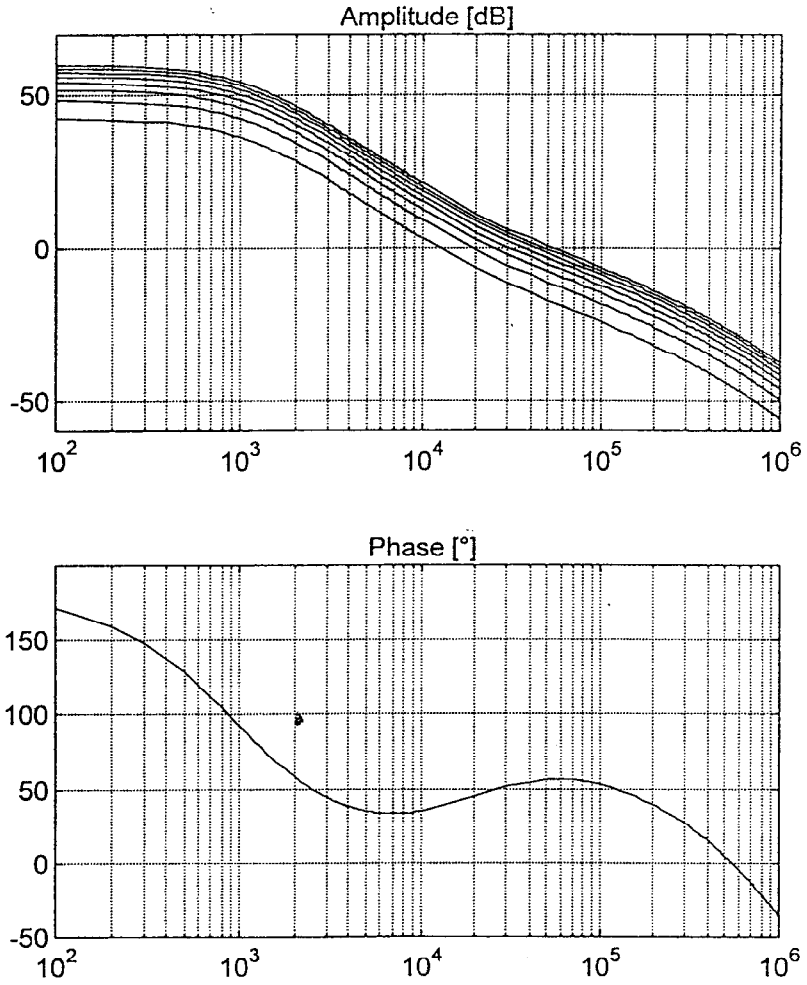

Figure 11 – Amplitude and phase frequency responses

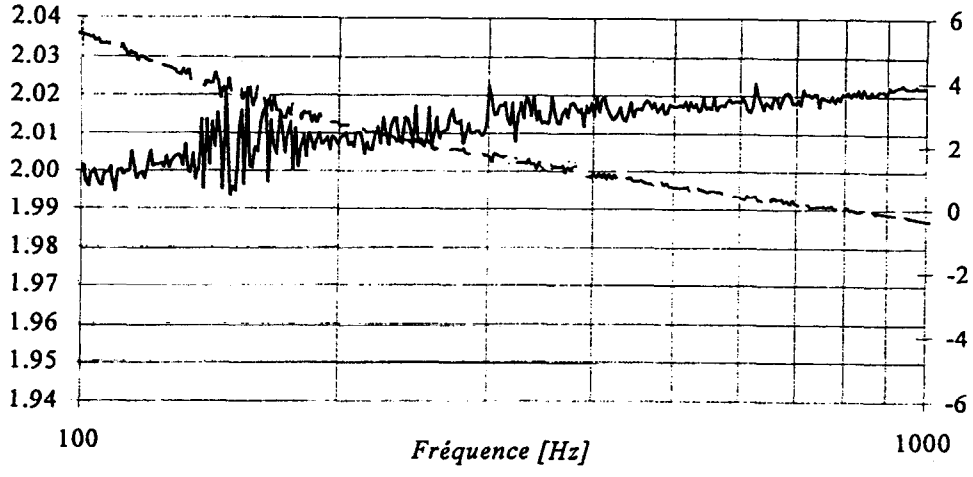

Figure 12 – Modulus and phase frequency responses of the transconductance

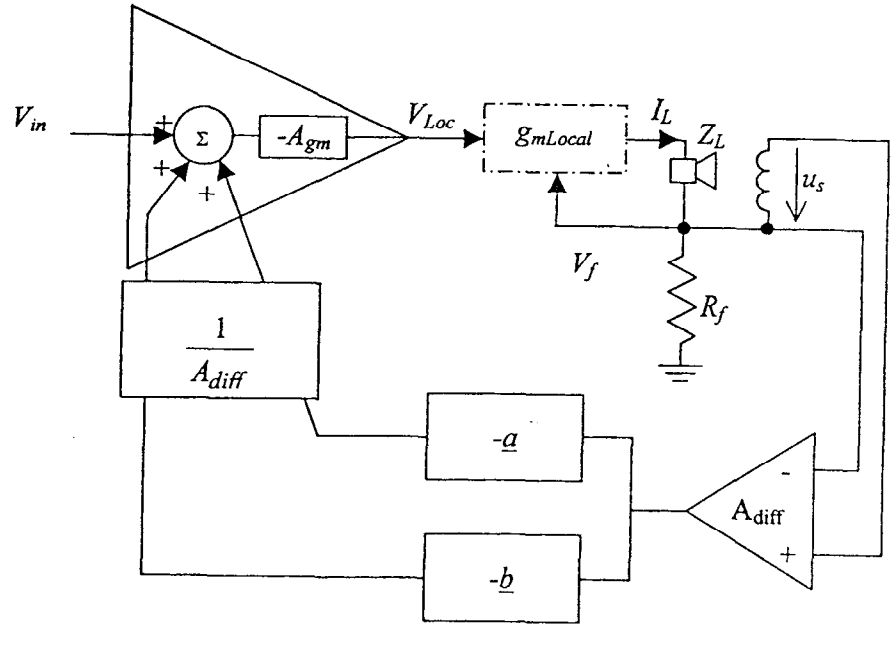

Figure 13 – Complete bloc diagram with feedback.
$\underline{a}$ et $\underline{b}$ are the velocity and acceleration gain factors

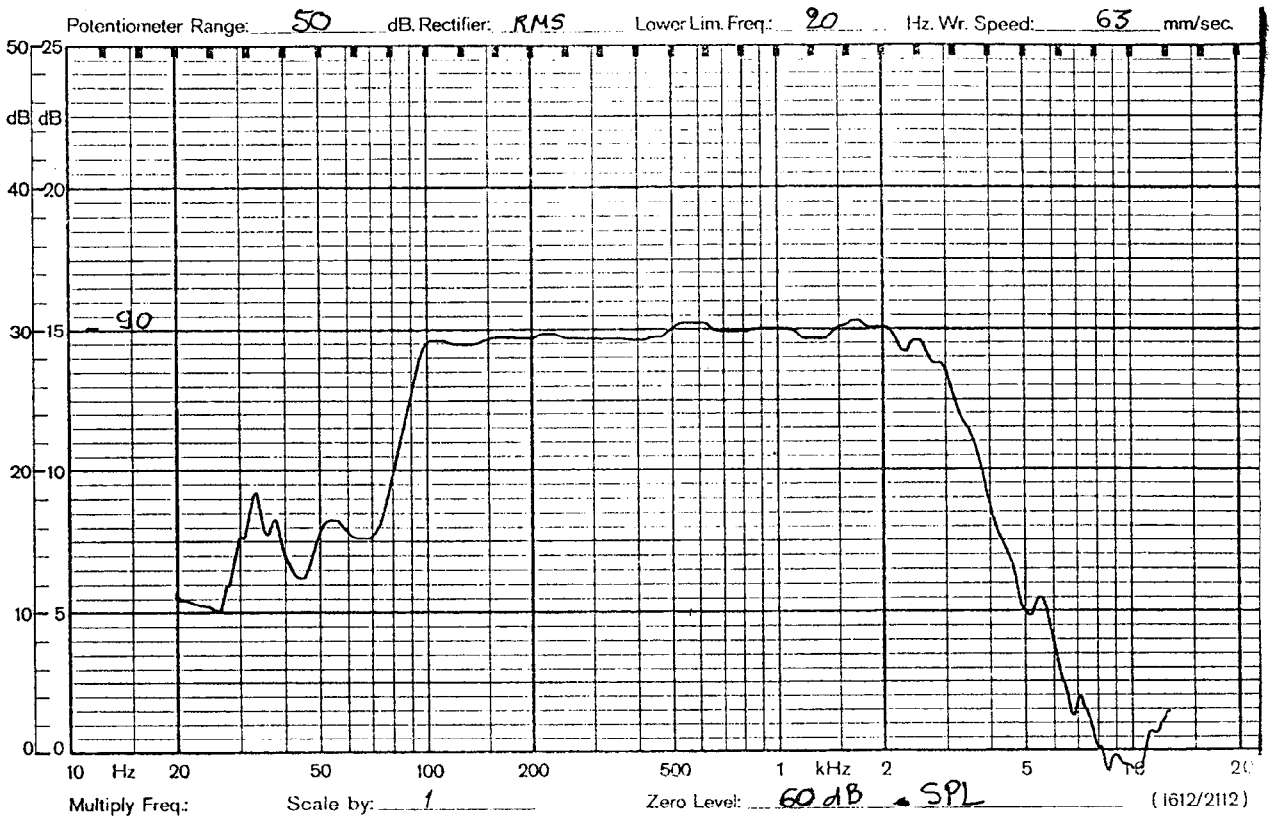

Figure 14 – Amplitude frequency response

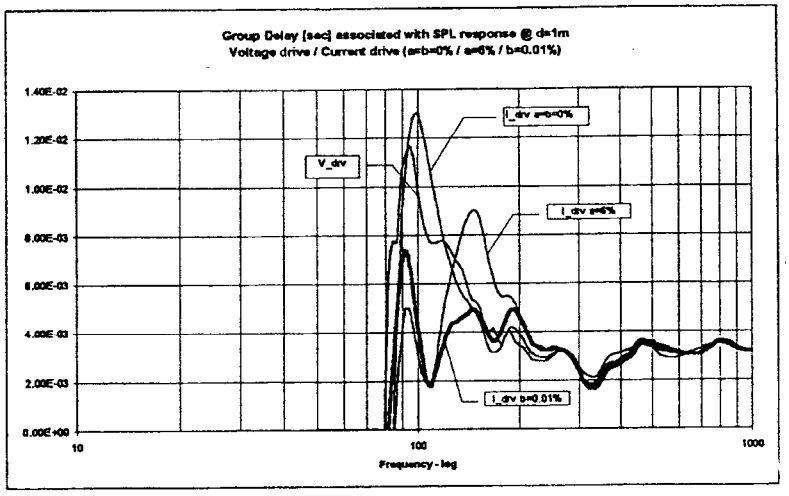

Figure 15 – Group delay curves

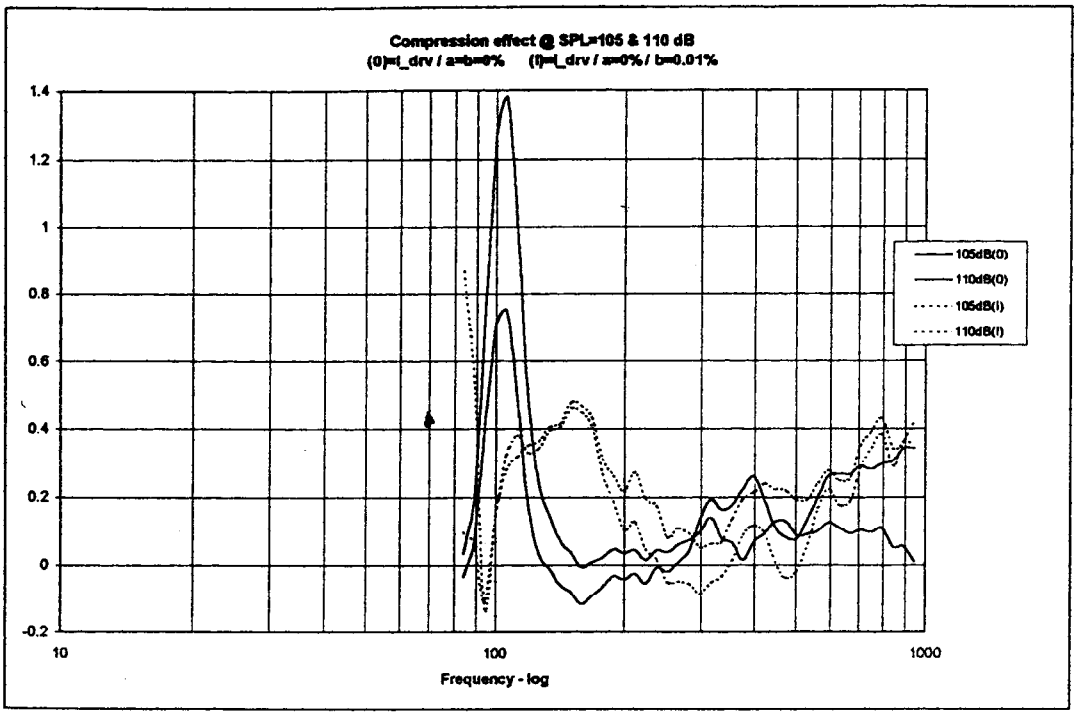

Figure 16 – Effects of compression with and without feedback

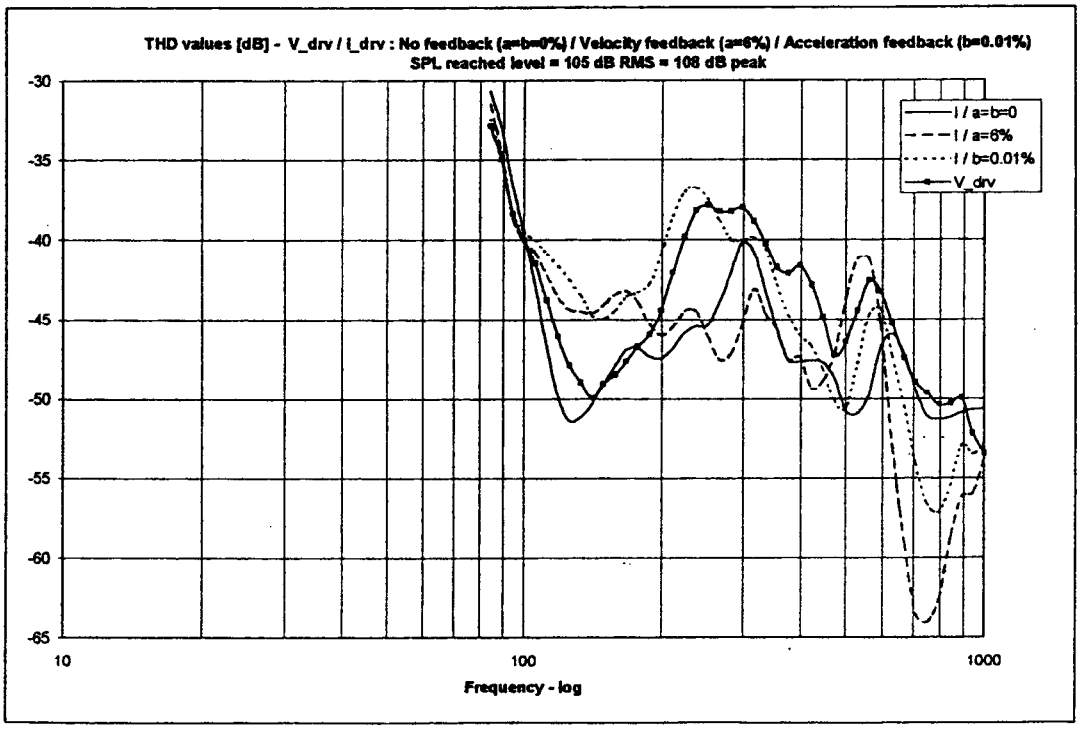

Figure 17 – THD at 105dB @ 1m for different controls

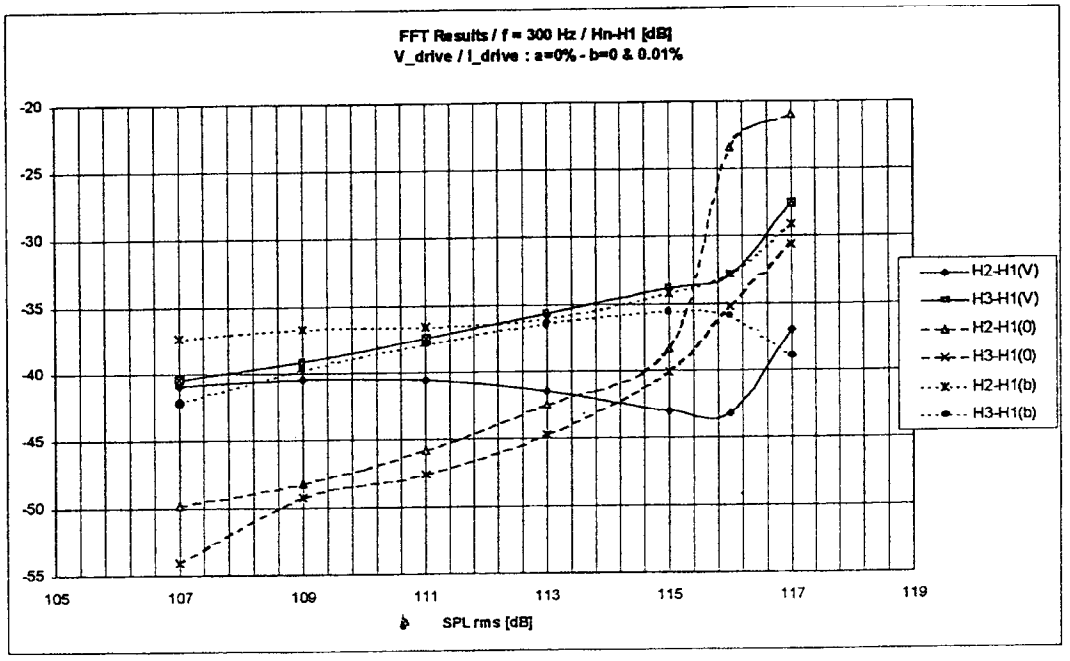

Figure 18 – THD 2nd and 3rd – measurements in bursts